# Formation of multilayered biopolymer microcapsules and microparticles in a multiphase microfluidic flow

Elisabeth Rondeau[1] and Justin J. Cooper-White[1,2,a)]
[1]*Tissue Engineering and Microfluidics Laboratory, Australian Institute for Bioengineering and Nanotechnology (AIBN), The University of Queensland, St. Lucia, Queensland, Australia*
[2]*School of Chemical Engineering, The University of Queensland, St. Lucia, Queensland, Australia*

(Received 1 March 2012; accepted 11 May 2012; published online 24 May 2012)

This paper reports the development of a scalable continuous microfluidic-based method for the preparation of multilayered biopolymer microcapsules and microparticles, with a size range of 1 to 100 $\mu$m, in a single-layered polydimethylsiloxane-based device. This new approach has been utilised to produce polyethylene oxide (PEO)-based microparticles, layered with subsequent stage wise coatings of polylactide-based block copolymers and polyvinylpyrrolidone. The production process was shown to allow for on-chip encapsulation of protein and vitamin molecules in the biopolymer micro particles, without any further handling after collection from the device. We have studied the release profiles in the case of model molecules of distinctive molecular weights, namely, vitronectin, horse radish peroxidase, and vitamin $B_{12}$. We compared the release properties of the microparticles to those from macro-gels of the same materials prepared off-chip. The results indicated that the microparticles have definitively different molecular weight cut-off characteristics, likely due to a denser microstructure within the microparticles compared to the bulk hydrogels. This difference suggests that significant benefits may exist in the use of this method to produce layered biopolymer microparticles in achieving improved controlled release and encapsulation. © *2012 American Institute of Physics*.
[http://dx.doi.org/10.1063/1.4722296]

## I. INTRODUCTION

Biopolymer-based microparticles, produced by a number of processing routes, for example, emulsification and solidification, are commonly utilised as controlled release vehicles in food, pharmaceutical, agricultural, and personal care applications.[1–3] Factors affecting the efficacy of active (e.g., drug) release from such particle systems, which include both the physical and the chemical properties of the base polymer,[1] as well as the physical properties of the resultant microspheres (such as their size,[4] size distribution,[5] morphology,[6] and porosity[7]), are all highly dependent on the method of preparation. Further, the variability of the environments in which the microparticles must deliver their payload, for example, to different locations in the gastro-intestinal (GI) tract, may also require the inclusion of a variety of "release" triggers[8–10] within such microparticles or further surface functionalization of the microparticles, in order to enhance specificity for a desired target delivery site.[11]

Developments in microfabrication techniques and microreaction technologies, coupled with the development of new microfluidic approaches[12,13] for preparing monodisperse water droplets in oil have recently enabled the production of monodisperse polymer-based microparticles (from both biologically derived[14–17] and synthetic polymers[18–22]). In the first processing stage

a)Author to whom correspondence should be addressed: Electronic mail: j.cooperwhite@uq.edu.au. Tel.: +61 7 3346 3858.

 

of such devices, a monomer or a polymer solution is emulsified using either T-junction[12,23,24] or by flow-focusing[25] geometries to produce highly monodisperse droplets, with the droplet size being controlled by the relative flow rates of each phase, the viscosities of each phase and the interfacial tension between the two phases. Monomer droplets are then solidified by means of thermally initiated[26] or UV-initiated batch polymerization.[27] In addition, these processes lend themselves to cross-linking of synthetic polymers, where droplets of polymer solutions are hardened by either solvent evaporation,[28–30] by physical or photo-initiated cross-linking,[31] or by means of chemical reactions.[32] The particles derived from this process scheme are typically a few hundred micrometres in diameter, with very little deviation in size (<5%).

The production of polymer microspheres and microcapsules from biologically derived polymers using microfluidic processes has also been recently reported in the literature.[33] Huang *et al.*,[15] for example, used a microfluidic device to generate Na-alginate microspheres, which were subsequently dripped (off-chip) into a solution containing calcium ions to form Ca-alginate microspheres. They studied the entrapment efficiency of these microspheres, using gold nanoparticles as a model drug, to confirm the potential of such a production technique for encapsulation applications. De Geest *et al.*[34] reported the synthesis of microgels from dextran-hydroxyethyl methacrylate droplets pre-formed in a microfluidic device and photo-polymerized after collection from the chip. The resulting microspheres were monodisperse, with a diameter of approximately 10 $\mu$m. However, similar to the limitations experienced in biopolymer microbead manufacture using non-microfluidic-based techniques, the production of polymer beads via the aforementioned two-step processes fails to realize the full potential of continuous microfluidic-based synthesis.

Several studies have more recently described the development of microfluidic reactors designed to allow the emulsification via rapid droplet formation and synthesis of polymer particles in one device. The preparation of polymer particles with different compositions via photopolymerisation of acrylate-based droplets in the constrained geometry of microfluidic devices was demonstrated and explored: particles with varying size,[20,35,36] shape,[19,37] morphology,[21] and composition[38] were synthesized. The strategy was extended to the continuous synthesis of redox polymerized microgels,[39] biodegradable microparticles,[16] and biopolymer microcapsules.[14] These works have certainly secured microfluidic-based approaches as a way to overcome the limitations of standard (bulk) microparticle production methods. However, in general, further optimization of microfluidic reactors for superior control over the size and size distribution of the produced particles, inclusive of compositional flexibility and surface functionalization, is still required.

With this challenge in mind, we investigated the possibility of using microfluidic device technology to produce multilayered particles from multiple different polymers in a single-step process, building on a simple device design utilised previously to produce single biopolymer micro- and nano-particles.[40] The core of these multilayered particles was made from acrylated Pluronic (PEO-PPO-PEO) polymers.[41] The deposition of a single polymer layer and of two successive polymer layers onto this pluronic-based core was then successfully integrated into one microfluidic device design. We have investigated the influence of the device geometry, flow parameters, and polymer solution properties on droplet generation and multilayered particle formation. This microfluidic-based method was thereafter shown to efficiently encapsulate a number of deliverables including vitamin B and protein (horse radish peroxidase (HRP) and vitronectin) molecules. The study of the release properties of the particles showed that differences in the microstructure of the cross-linked core and multilayered particles, when compared to the bulk hydrogel, result in different molecular weight (or size) cut-offs, offering the potential for controlled delivery of two molecules of differing size over two vastly different timescales.

## II. EXPERIMENTAL SECTION

### A. Materials

#### 1. Monomers and polymers

Pluronic F-127, ($EO_{100}PO_{70}EO_{100}$) (PF-127), Pluronic F-68 ($EO_{80}PO_{30}EO_{80}$) (PF-68), and 1-Vinyl-2-Pyrrolidone (MVP) were purchased from Sigma-Aldrich (NSW, Australia). Polylactide

(PLA)-based block copolymer ($PLA_{4700}PEO_{5100}PLA_{4700}$) was purchased from Polymer Source (Montréal, Canada).

#### 2. Reagents

Acryloyl chloride, triethylamine, ethylene glycol dimethacrylate (EGDMA), 2,2′–Diethoxyacetophenone (DEAP), ammonium persulfate (APS), and N,N,N',N'-tetramethylenediamine (TEMED) were purchased from Sigma Aldrich (NSW, Australia). 2,2′-Azobis (2-amidinopropane) dihydrochloride (Vazo®56) was purchased from DuPont (Saint-Louis, MO, USA). Alexa Fluor® 488 dye was purchased from Invitrogen (QLD, Australia). Vitronectin (VN) from human plasma was obtained from Promega (WI, USA). Polyclonal rabbit anti-human VN was purchased from Calbiochem (Germany) and HRP-conjugated goat-anti-rabbit IgG from Novagen (WI, USA). HRP, Vitamin $B_{12}$ ($VB_{12}$), Tween 20, and 2,2′-azino-di-[3-ethyl-benzothiazoline-6 sulfonic acid] diammonium salt (ABTS) were purchased from Sigma Aldrich (NSW, Australia).

#### 3. Solvents and buffer solutions

Anhydrous dimethyl carbonate (DMC) was purchased from Sigma Aldrich (NSW, Australia). All buffer solutions for the sandwich enzyme-linked immunosorbent assay (ELISA) were prepared in phosphate buffered saline (PBS) and tris buffered saline (TBS) solutions.

### B. Methods

#### 1. Diacrylation of Pluronic polymers and cross-linking reaction

Synthesis of di-acrylated (DA) pluronic DA PF-127 and DA PF-68 followed previously described methods in the literature.[41–43] Briefly, hydroxyl groups of PF-127 or PF-68 were acrylated by reacting dried polymer and a 10-fold molar excess of both acryloyl chloride and triethylamine in anhydrous dichloromethane, which was allowed to stir under argon overnight. The resulting polymer was then precipitated in cold anhydrous diethyl ether, filtered, and dried under a vacuum for 3 to 4 days. The obtained polymer was analysed in deuterated water, using 500 MHz $^1$H-NMR on a Bruker Advance 500 high-resolution NMR spectrometer, which confirmed the presence of the acryl protons at 5.8–6.4 ppm. The degree of acrylation was found to be systematically above 95% for both DA PF-127 and DA PF-68. For all experiments, including the production of the particles, DA PF-127 and DA PF-68 solutions with concentrations ranging from 5% to 20% (w/w) and 15% to 25% (w/w), respectively, were prepared in deionised water (Millipore r = 18.2 M Ω cm at 26.2 °C).

Cross-linking of DA PF-127 and DA PF-68 was initiated using two alternative systems: Vazo®56 and UV-light or APS and TEMED. In the case of the redox-initiating system (APS + TEMED), the kinetics of the cross-linking reaction were studied by observing the changes in rheological properties during the formation of the gel, using a controlled stress rheometer (ARG2, TA Instruments) with a cone-plate geometry (40 mm, 2°).

#### 2. Fabrication of the microfluidic reactor

The design of the microfluidic device or reactor used for the formation for the single core and multilayered particles and the typical dimensions of the channel at the droplet formation zone are shown in Figures 1(a) and 1(b). The microchannels were either 100 $\mu$m or 200 $\mu$m deep. Masters were prepared from SU-8 photoresist (MicroChem, USA) in bas-relief on silicon wafers. Microchannels were fabricated from Sylgard Brand 184 Silicone Elastomer (Dow Corning), using a standard soft-lithography method, which allowed rapid replication of the integrated microchannel prototypes. The polydimethylsiloxane (PDMS) devices were mounted on glass or quartz slides for use on the inverted fluorescent microscope (TE2000, Nikon).

#### 3. Particle preparation: Experimental setup

Gas-tight microsyringes (S.G.E) were filled with the polymer solutions and mounted on a motor-driven syringe pump (PHD 2000 Harvard, Instech), which could synchronously operate

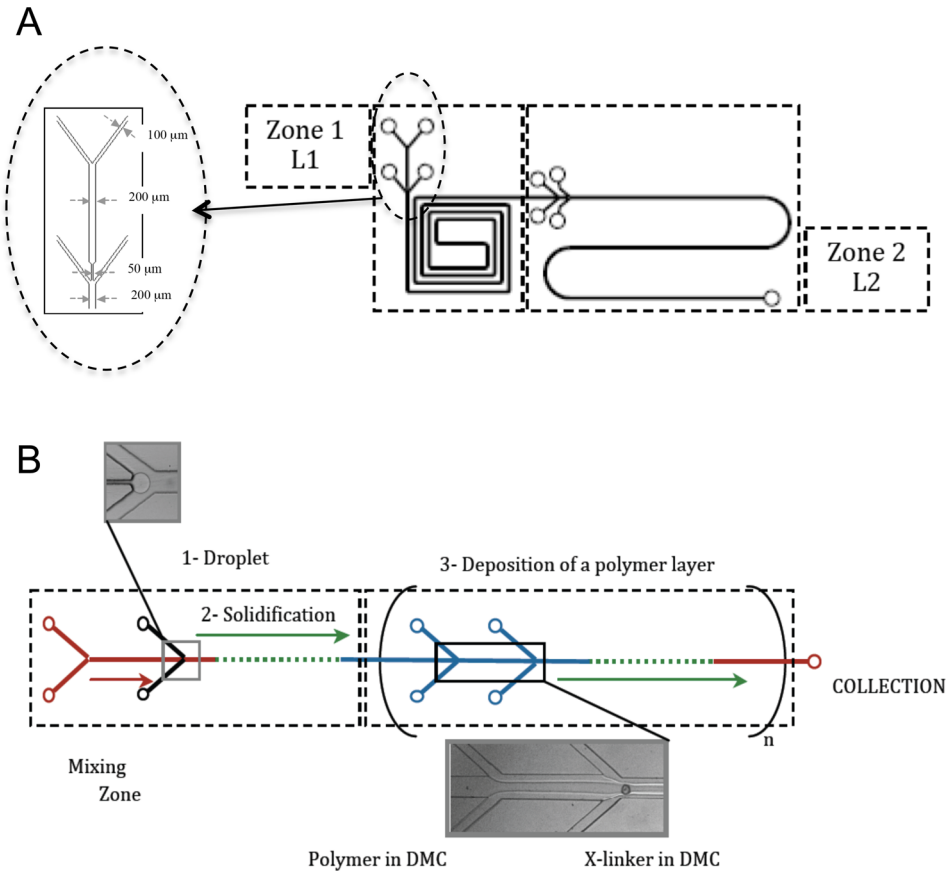


FIG. 1. (a) Schematic of the microfluidic flow focusing geometry used for the continuous production of single and multi-layer biopolymer microparticles. Insert—corresponding dimensions of flow-focusing section. (b) Schematic showing regions of the microfluidic device: droplet formation, solidification and deposition of a single (coating) layer.

two syringes at various flow rates. The PDMS device was linked to these syringes with polyethylene tubing (I.D. 0.58 mm/O.D. 0.965 mm). The resulting particles, dispersed within the continuous phase, were collected from the device via another segment of polyethylene tubing (PE50, Intramedic). Images of droplet formation and shrinkage were captured and processed using a high-speed camera (Phantom V, Vision Research), which can capture up to 64 000 fps at $256 \times 256$ pixels resolution, attached to a Nikon inverted microscope (TE2000, Nikon) coupled with a phase contrast condenser. Frame rates used in the experiments reported here were varied from 1000 fps to 2000 fps, and the exposure time was approximately 130 $\mu$s.

### 4. Encapsulation of deliverable molecules in the microparticles

The encapsulation of VN, HRP, or $VB_{12}$ in the particles was processed within the same device. The molecules to be released were mixed in the polymer solution before being injected via the syringe in the device. This did not affect the viscosity of the disperse phase and droplets of aqueous polymer solution containing the water-soluble protein, enzyme, or vitamin molecules were generated following the same process as that used with no deliverables present.

### 5. Evidence of entrapment

Vitronectin molecules were coupled with a green-fluorescent Alexa Fluor 488 succinimidyl ester (AF 488) prior to encapsulation. The labelled protein molecules were encapsulated in Pluronic cross-linked particles produced on-chip. The resulting particles were collected from the device and observed using a motorized inverted microscope Olympus IX81, with a

phase-contrast objective and a filter set DAPI/FITC/TexasRed (excitation filter BP 492/18, U-MF2 filter cube with DAPI/FITC/TexasRed triple band dichroic mirror and emission filter) for fluorescence microscopy.

#### *6. Release studies*

After collection from the device, the particles were dried by allowing the DMC evaporate in a dessicator, at room temperature. The beads were thereafter re-suspended in a known volume of PBS. The suspension was kept at room temperature. A small volume of the supernatant was sampled at desired time points. The VN, HRP, or $VB_{12}$ content in the supernatant was determined using different assays, as described below, and the percentage of release was expressed in terms of percentage, with respect to initial loadings.

*a. Detection of vitronectin.* An indirect ELISA protocol was used to quantify the concentration of vitronectin in the supernatant solution. This technique has a limit of detection of $\sim 0.5$ ng/ml VN in 100 $\mu$l (i.e., 50 pg VN). Polyclonal rabbit anti-human VN was used as the primary antibody and HRP-conjugated goat-anti-rabbit IgG as the second antibody. ABTS was used as a substrate and after it is added, a green color develops indicating the presence of bound second antibody. The VN concentration was then measured by an absorbance plate reader at 405 nm.

*b. Detection of HRP.* The concentration of HRP in the supernatant solution was measured by absorbance at 405 nm, using ABTS as a substrate.

*c. Detection of vitamin $B_{12}$.* Vitamin $B_{12}$ absorbs at 361 nm. A simple measurement on an absorbance plate reader allowed quantification of the concentration of VB12 in the sampled solution.

## III. RESULTS AND DISCUSSION

### A. Investigation of the cross-linking reaction of diacrylated Pluronic polymers DA PF-127 and DA PF-68

The formation of chemically cross-linked gels from diacrylated pluronic can be obtained via a photo-curing[44–46] or via a redox-initiated reaction.[47] In order to compare the duration of the cross-linking reaction with the residence time of the droplets/particles within the microfluidic channels (discussed in Sec. III B), we conducted preliminary experiments on aqueous solutions of DA PF-127 and DA PF-68 for both initiating systems. Ideally, the cross-linking reaction occurs instantaneously, preventing any breakage or coalescence of the droplets as they flow within the channel after they are generated. By the time, they are collected from the device, the particles have to be stable upon dilution and withstand environmental changes and shear forces without any structural deterioration.

We firstly investigated the kinetics of the *redox-initiated* cross-linking reaction for DA PF-127 and for DA PF-68 aqueous solutions using rheometry. The evolution of the viscoelastic properties of the polymer solutions as the cross-linking reaction progressed was monitored using oscillatory shear measurements. Figure 2 shows the comparison of the evolution of the storage modulus (G') with time after mixing APS + TEMED to the DA pluronic solutions, in the case of DA PF-68 solutions with varying polymer concentration and varying TEMED concentration, but with the same APS concentration. There was no significant effect of the APS concentration on the induction times or duration of cross-linking (data not shown). Figure 2 shows that the elastic modulus increases with time as the covalent gel forms. The final equilibrium modulus was highly sensitive to the Pluronic concentration. G' reaches a plateau at around 30 kPa for the 15 wt. % solution and at around 50 kPa for the 20 wt. % solution. Aqueous Pluronic solutions are known to show thermo-reversible gelation behaviour and the gelation temperature depends on the polymer concentration, but in the case of non-acrylated PF-68, no gel is observed at room temperature for concentrations as low as 15 or 20 wt. %. The increase

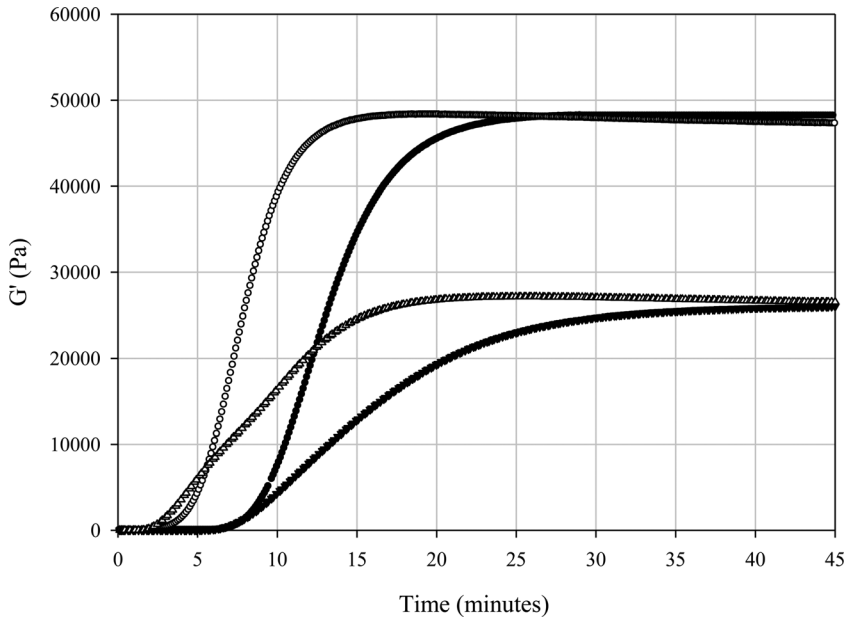


FIG. 2. Evolution of storage modulus as a function of time during the redox-initiated cross-linking reaction of F68DA 15 wt. % aqueous solution (triangles) at 40 rad/s and 10% strain and 20wt. % solution (spheres) at 40 rad/s and 15% strain. The induction time of the reaction varies when decreasing the concentration of accelerator (TEMED) in the original reactive solution from 30 ml/g(DA PF-68) (open symbols) to 15 ml/g(DA PF-68) (filled symbols). The concentration of APS is the same for all initial reactive solutions: 4% (w/w(DA PF-68)). There is no effect of the amount of TEMED on the final modulus.

in G' and G" after the addition of the initiators, in the case of the reactive DA PF-68 solution, is thus due to the final cross-linked gel structure, as determined by the initial packing state of acrylated Pluronic macromers, which was found to be highly dependent on the polymer concentration.

For a given DA PF-68 concentration, the induction time and the reaction duration are decreased with increasing TEMED concentration. Similar results were found for DA PF-127 solutions (data not shown). The reaction induction time was between 2 and 3 min, which is significant compared to the usual residence times in the microdevice, at the flow rates typically explored in this work. The hardening of the droplet needs to occur within the device, before collection of the particles.

We also conducted preliminary tests in the case of the photo-induced cross-linking reaction. Small volumes of DA PF-127 and DA PF-68 aqueous solutions of varying polymer concentration were mixed with various amounts of the photo-initiator and irradiated under the same UV-lamp as used for the production process on-chip (see Sec. III B). These tests allowed for the elucidation of the time required for the formation of a uniform gel for each experimental condition. Adjusting the initiator concentration, the cross-linking reaction was observed to occur after 20 to 30 s for relatively low DA Pluronic concentrations (10 wt. % for DA PF-127 and 15 wt. % for DA PF-68). In general, for a given DA Pluronic concentration, due to the substantial induction time for the redox-initiated reaction, the photo-induced reaction was found to be faster than that of the redox-initiated reaction.

### B. Preparation of cross-linked coated particles within the microfluidic device

As presented in Figure 1(b), the channel network used in the present work consists of three functional parts: a sheath-flow junction (1), where droplets are formed, a serpentine channel (2), in which the droplets harden and flow-focusing devices (3), for the subsequent deposition of additional polymer layers.

### 1. Mixing zone

We investigated both the redox-initiated cross-linking reaction and the photo-induced reaction within the microfluidic device. The device design, as presented in Figures 1 and 3, allows reactive mixtures to be processed upstream of the microdroplet creation site. In the case of the redox system, the TEMED, which is an accelerator, is mixed with the DA pluronic solution prior to injection. The resulting polymer solution and the solution containing the APS are individually injected side-by-side at the same flow rate in the device and they mix within the channel to form the dispersed phase. The length of the mixing channel is typically 10 mm. The residence times for flow rates of 5 $\mu$l/h to 10 $\mu$l/h ranges from approximately 5 min down to 2 min.[40]

The aforementioned rheological study showed that the induction time before the start of the formation of a gel is typically from 2 min to 7 min for the redox-initiated reaction. If the two solutions are assumed to be homogeneously mixed together at the end of the mixing zone, the cross-linking reaction will not have occurred prior to droplet formation.

In the case of the photo-induced reaction, the DA pluronic solution and the V56 solution are individually injected. They mix to form the disperse phase in the same mixing zone, which is protected from the UV light to avoid initiating the cross-linking reaction before droplet formation. This would lead to an increase in the viscosity of the polymer dispersed phase and potentially prevent the generation of the pre-polymer droplets. In all cases, the viscosity of the disperse phase was low enough to allow for the continuous production of droplets.

### 2. Droplet formation

The reactive disperse phase, consisting of the DA polymer and the cross-linker solutions, is assumed to be homogeneously mixed by the time they reach the sheath junction. For a given solution with a certain viscosity, the droplet size and the break-up frequency are dependent on the flow rates of the dispersed and the continuous phases ($Q_D$ and $Q_C$, respectively). The droplet

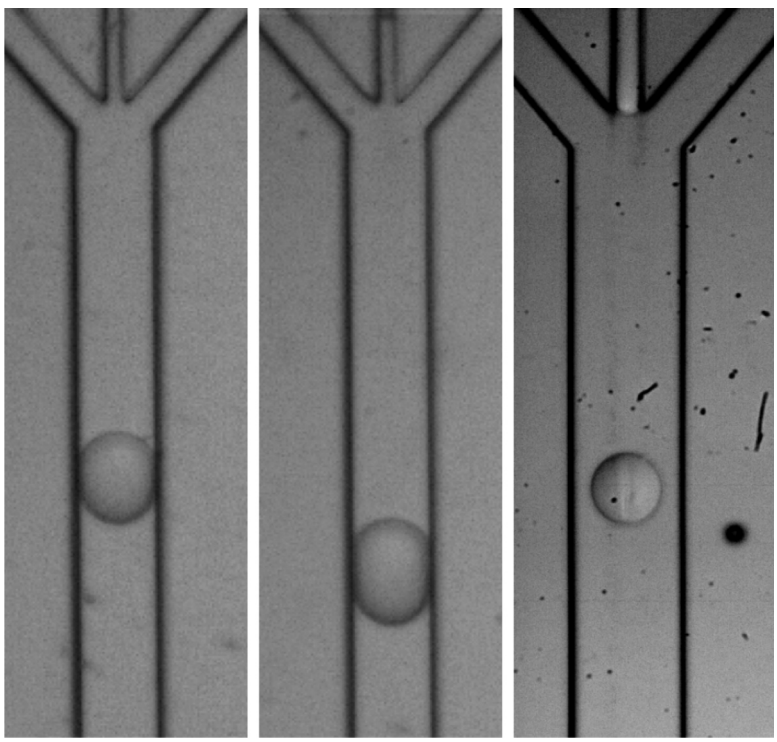

FIG. 3. Images showing differences in droplet size as a function of flowrates of continuous and dispersed phases. (a) $Q_C = 0.5$ ml/h, $Q_D = 2$ ml/h, (b) $Q_C = 0.5$ ml/h, $Q_D = 6$ ml/h, (c) $Q_C = 1$ ml/h, $Q_D = 8$ ml/h.

size depends on both $Q_D$ and $Q_C$. The variation of the mean droplet size is traditionally plotted as a function of the disperse phase $Q_D$, at a fixed $Q_C$,[48] or as a function of the continuous phase flow rate $Q_C$, at a constant $Q_D$.[14] The droplet size was shown to increase with increasing $Q_D$ and to decrease with increasing $Q_C$. Figure 3 shows images of droplets generated using three different flow rate conditions: at $Q_C = 0.5$ ml/h and $Q_D = 2$ $\mu$l/h, at $Q_C = 0.5$ ml/h and $Q_D = 6$ $\mu$l/h, and at $Q_C = 1$ ml/h and $Q_D = 8$ $\mu$l/h.

The comparison of these images shows that the droplet is larger at a higher $Q_D$, for the same $Q_C$, but it is smaller at higher $Q_D$, and a higher $Q_C$. This data confirm that for these particular polymeric systems, the droplet size can be tuned by adjusting the ratio $Q_C/Q_D$. In this study, the domain in which DA Pluronic droplets were produced at a constant frequency and of uniform size covered a large range of flow rates. Typically, $Q_D$ could be varied over a range of 5 $\mu$l/h to 10 $\mu$l/h and $Q_C$ over a range of 0.7 ml/h to 1.2 ml/h. After setting $Q_C$ to achieve the desired total residence time for the reactive mixture to obtain cross-linked microgels within the device, $Q_D$ was manipulated to tune the droplet size.

### 3. Cross-linking reaction/hardening of the droplets

*a. Redox-induced cross-linking reaction.* Once the microdroplets come into contact with the DMC continuous phase (i.e., post the initial creation of an interface), post the sheath focusing junction, they shrink. This causes a reduction in size of the particles as they solidify and flow downstream in the device. This phenomenon and the competing processes have been previously described.[40] As the droplets shrink, the polymer concentration changes inside the droplets, and as a result, the time for the cross-linking reaction to come to completion decreases. Table I shows the residence time corresponding to the length of the main channel. The two zones (Zone 1 and Zone 2) are displayed in Figure 1(a).

The droplets are flowing for 14 s or for 28 s, depending on $Q_C$, in Zone 1, until the droplets/particles reach the site where another polymer solution, to be deposited on their surface, is injected via co-flowing channels. The particles remain in the device for 13.5 to 27 more seconds after this point, in Zone 2. In the case of the redox-initiated reaction, the reactive droplets contain the DA Pluronic, the APS and the TEMED. The duration of the cross-linking reaction when studied off-chip was found to be much longer than the longest residence times of the droplets in the device, yet due to the particles shrinking as they flow downstream, carried by the DMC, the local increase in the polymer concentration must allow for the solidification process to come to completion in the device, as the particles are solidified on exit from the channel. In addition, internal recirculation within the droplets could also be responsible for increased local mixing and hence reduced kinetics of crosslinking, however, as polymers (or solution elasticity) are known to substantially effect the dynamics of recirculation vortices in microchannels, further work is required to confirm the actual reason for these observed differences. After collection, the particles were observed to be only a few microns in diameter. Figure 4 shows SEM and TEM images of the resulting particles. They have a core-shell structure, which suggests that the microparticles are not uniformly gelled, the dark core corresponding to a higher cross-linking density.

*b. UV-induced cross-linking reaction.* Exposure of a section of the channel with a UV lamp (from underneath) was utilised to initiate the cross-linking reaction in the droplets

TABLE I. Residence times of the droplets/particles in the channel, as a function of the flow rate of the continuous phase ($Q_C$), in Zone 1 and in Zone 2 (see Figure 5 for partition).

| | L1 = 130 mm | L2 = 125 mm | L1 + L2 |
|---|---|---|---|
| $Q_C = 0.5$ ml/h | 28 s | 27 s | 55 s |
| $Q_C = 0.6$ ml/h | 23.5 s | 22.5 s | 45 s |
| $Q_C = 0.8$ ml/h | 17.5 s | 17 s | 34.5 s |
| $Q_C = 1$ ml/h | 14 s | 13.5 s | 27.5 s |

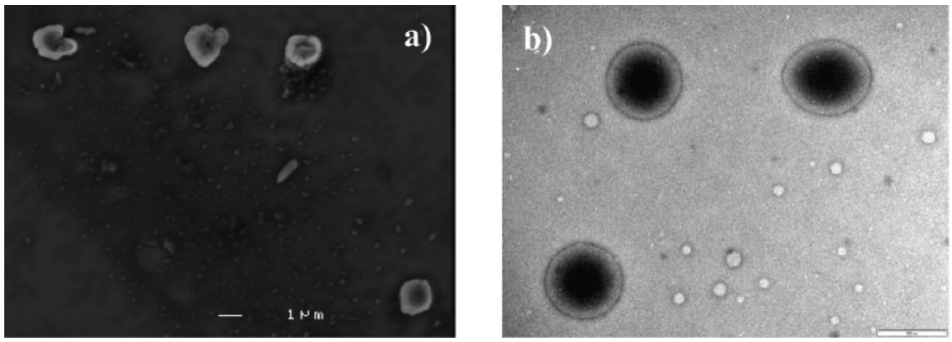


FIG. 4. (a) SEM image of DA F-127 cross-linked microparticles produced on-chip via a redox-initiated reaction. The particle size is approximately 1 $\mu$m. (b) TEM images of the same system. Note the dense core and diffuse shell.

composed of the DA Pluronics and the V56 initiator. Using a UV-Visible spectrophotometer, we measured the absorption spectrum for V56 dissolved in water. As presented in Figure 5, the corresponding spectrum shows a very narrow peak with a maximum absorption for wavelengths in a range from 180 to 220 nm. Glass slides commonly used for microfabrication were found to absorb all light below 300 nm. To allow UV light to pass through into the device and initiate crosslinking of the microdroplets flowing in the channel, the PDMS device was mounted on a quartz slide.

Figure 6(a) shows a cross-linked particle flowing in the channel. The image reveals an open shell-like structure, with polymer as the outer phase and a hollow centre. This was observed for both DA PF-68 and DA PF-127, in a reproducible manner. Figure 6(b) shows images of cross-linked DA-PF127 particles, made via the UV-induced route, collected from the device and deposited on a microscope slide to allow the DMC to evaporate. The particles are highly monodisperse and have a diameter of approximately 80 $\mu$m. Figure 6(c) shows SEM images of cross-linked DA PF-68 and DA PF-127, respectively, produced using the same process parameters, collected from the device and dried. These images confirm the shell-like structure for both materials. They are highly monodisperse and have diameters of 60 and 80 $\mu$m, respectively. This shell-like structure is unusual, considering that such a structure was not observed for the redox-initiated reaction. We know that the hardening of the droplets within the

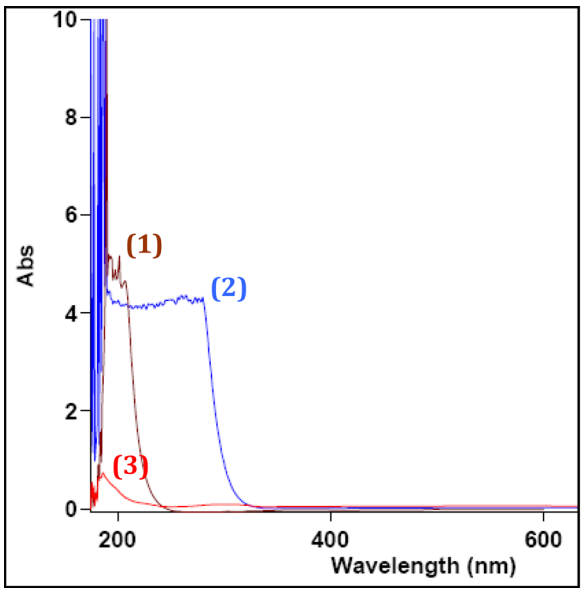


FIG. 5. Absorption spectra for (**1**) V56 in DI water, (**2**) a glass slide, (**3**) a quartz slide.

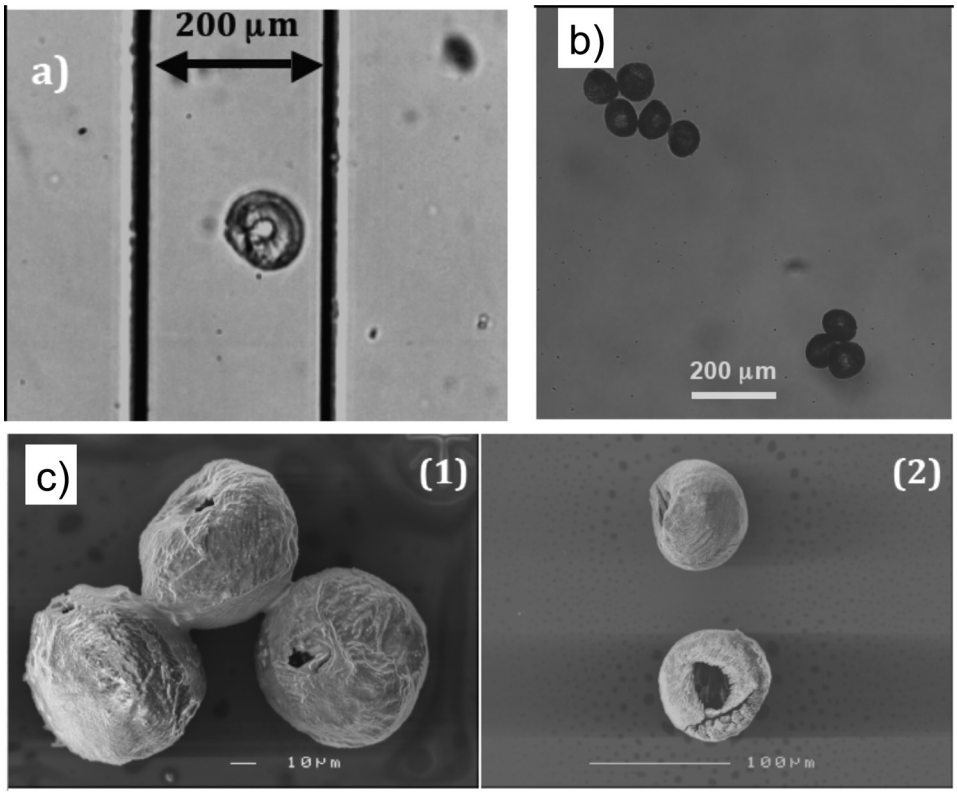


FIG. 6. (a) Optical microscopy image of a DA PF-127 capsule flowing in the channel post UV initiation, showing the formation of a shell of different density to the centre of the particle. (b) Optical microscopy images of DA PF-127 photo cross-linked particles deposited on a microscope slide after collection from the device. (c) SEM images of DA PF-68 (1) and DA PF-127 (2) cross-linked microcapsules produced on-chip via a photo-initiated reaction. The particle size is approximately 60 and 80 $\mu$m, respectively.

microdevice will not be spontaneous, and that as they are flowing along the microchannel, due to the partial miscibility of the solvent (water) with the continuous phase (DMC), that the water is eluting out of the droplets, resulting in the polymer droplets shrinking. This will lead to a much higher local concentration of Pluronic chains at the sub-phase between the water and DMC, which when coupled with the inherent surface activity of Pluronic polymers, could certainly rise to the shell-like particles observed in these images. The reason for the "port-hole" in these microparticles (see, in particular, Figure 6(c)) is currently unknown.

### *4. Deposition of successive polymer layers within the same device*

Chu *et al.*[49] used a microcapillary technique to produce monodisperse multiple emulsions with high degrees of control over the size of the droplets formed at each stage of the process. They formed double and triple emulsions by successively breaking up the multiphase fluid with another immiscible fluid introduced via axisymmetric co-flowing capillaries. Based on a similar concept, we used a cascade of co-flowing channels for the injection of polymer or monomer solutions into the main channel, where the droplets/particles are carried along after they are generated upstream, within the same device. This allowed for the deposition of a thin layer of another polymer on the particle surface without interrupting the flow in the device at any time.

We assessed the deposition of a first layer onto formed particles using two different polymer systems; (1) triblock copolymers of PLA-PEO-PLA and (2) polyvinylpyrrolidone (PVP), via the photo-polymerization of 1-vinyl-2-pyrrolidone (MVP) using 2, 2'–diethoxyacetophenone as a photo-initiator. As shown in Figures 1(a) and 1(b), two sets of two axisymmetric co-flowing channels are used for the deposition of one layer. In the case of the PVP coating layer,

a solution of 2 wt. % MVP in DMC is introduced via the first of the two co-flowing channels (see Figure 7(a)) and only further downstream the DEAP is introduced (mixed into DMC) via the second of the two co-flowing channels. The channel downstream of both of these junctions is thereafter irradiated with UV light to allow for the polymerization of MVP molecules adsorbed on the surface of the DA Pluronic particle. The monomer concentration is very low and there is no noticeable viscosity change of the outer continuous phase as a result of the polymerization of the MVP still in solution.

In the case of the PLA-PEO-PLA coating layer, a 2 to 5 wt. % copolymer (in DMC) solution was introduced via the first two co-flowing channels and hexadecane was introduced further downstream, via the second set of channels, to convectively encourage closer contact of the block copolymer macromolecules to the surface of the particles. This is shown in Figure 7(b). Using a second set of four co-flowing channels, we deposited a second polymer layer onto these coated particles.

In all cases, the resulting particles or the microcapsules were collected via PE tubing. Figure 8 shows SEM images of cross-linked Pluronic microcapsules coated with a single layer of PLA-PEO-PLA or PVP, and of cross-linked PF-127 microparticles coated with a 1st layer of PVP and a 2nd layer of PLA-PEO-PLA. The surface morphology of the particles was observed to be different, depending on the nature of the outer layer. The deposition of PLA-PEO-PLA gave rise to rough surfaces, whereas PVP was observed to produce smoother surfaces.

### C. Encapsulation of desired actives within the device

One of the targeted applications for biopolymer microparticles and microcapsules produced utilizing the microfluidic processes described above is tailored delivery of protein molecules or other active substances. To assess the potential use of such particles as delivery vehicles, we encapsulated a number of model molecules of varying molecular weights, such as vitamin $B_{12}$ ($VB_{12}$), VN, or HRP. We have thereafter characterised the corresponding release profiles, comparing release properties of microgels prepared via this microfluidic-based process with those from bulk macrogels.

In order to show evidence of the encapsulation of vitronectin molecules in DA Pluronic cross-linked micro-capsules, fluorescently-labelled VN was mixed with the DA Pluronic solutions prior to injection into the microfluidic device. The *p*H of the polymer solution was adjusted to 3.5 with a few $\mu$l of a 1 M HCl solution to prevent the acrylate groups on the DA Pluronic macromolecules reacting with the thiol groups of the unpaired cysteines of vitronectin.[50,51] Aqueous droplets of the polymer mixture were formed and solidified in the same device. It has to be noted that the droplets/particles are surrounded at all times by a thin subphase of DMC-water and therefore the vitronectin never contacts the PDMS channel walls. The cross-linked particles were collected, dried, and suspended in a PBS solution. Figure 9 shows two images of cross-linked DA PF-127 particles containing vitronectin labelled with a green fluorescent dye, obtained, respectively, with a phase contrast objective and thereafter with FITC excitation and emission filters. In parallel, we conducted two control experiments with blank cross-linked DA

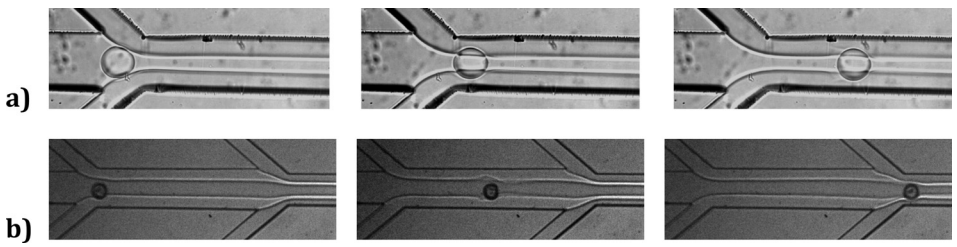


FIG. 7. (a) Axisymmetric co-flowing channel configuration for the introduction of a MVP solution into the main channel where DA PF-127 droplets/particles are flowing. The two continuous phases are partially miscible and do not diffuse into each other instantaneously. A DEAP solution in DMC is introduced further downstream. (b) A solution of 2 wt. % PLA-PEO-PLA in DMC is introduced via the first set of co-flowing channels and hexadecane is introduced via the second flow-focusing junction to push down the polymer solution onto the surface of the particles.

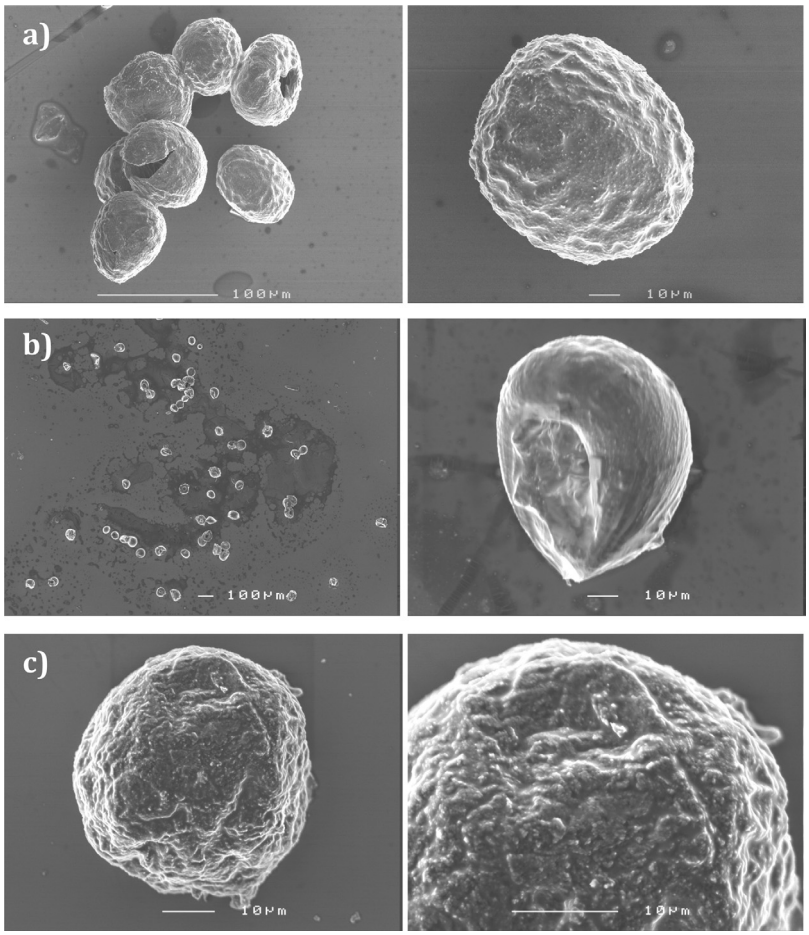


FIG. 8. SEM images of (a) DA PF-68 cross-linked microcapsules coated with PLA-PEO-PLA, (b) DA PF-127 cross-linked microcapsules coated with PVP, (c) DA PF-127 cross-linked microparticles coated with a 1st layer of PVP and a 2nd layer of PLA-PEO-PLA.

PF-127 particles and cross-linked DA PF-127 particles encapsulating unlabelled vitronectin molecules, to confirm if the reagents used in the process were auto-fluorescent, in the wavelength window of interest. The fluorescence microscopy images did not show any fluorescence for both control samples. This confirms that the particles in Figure 9 contain vitronectin molecules. The continuous phase (DMC), in which the particles are collected from the device, was also analysed

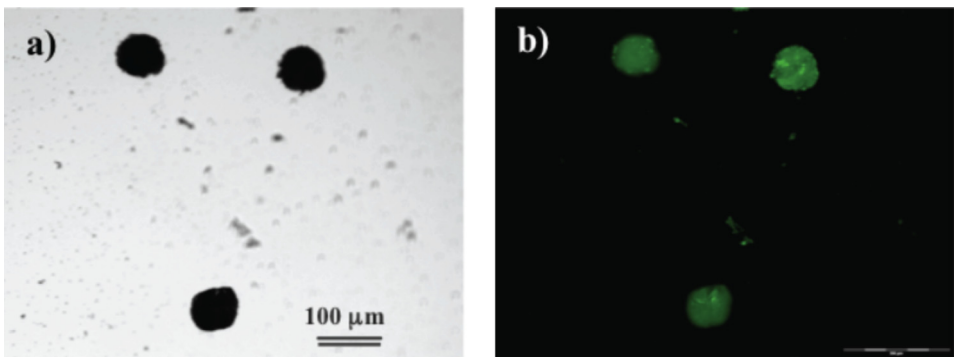


FIG. 9. Images obtained with an inverted microscope Olympus IX81 using (a) a phase contrast objective and (b) a green fluorescent filter.

with fluorescence microscopy. No fluorescence was detected, indicating that there was no significant loss of protein out of the droplets/particles during the encapsulation and solidification process.

## D. Delivery data

### *1. Release from Pluronic UV-cross-linked macrogels*

Macrogels were prepared from diacrylated Pluronic solutions, cross-linked via the same UV-initiated reaction as those processed in the microfluidic devices to form cross-linked Pluronic microparticles. Vitronectin, horse radish peroxidase, and vitamin $B_{12}$ molecules were, respectively, encapsulated in the UV-cross-linked PF-127 Pluronic gels by pre-mixing the substance of interest in the reactive polymer solution before processing the cross-linking reaction. The release was then studied for each species (VN, HRP, and $VB_{12}$), in order to investigate the effect of the size of the encapsulated molecules on the release profile. These results are shown in Figure 10.

The comparison clearly shows that the larger VN and HRP molecules (44 and 65 kDa, respectively) are released slower than the smaller $VB_{12}$ molecules. The profiles corresponding to VN and HRP are similar. It has to be noted that, when repeating the same "encapsulation and release" experiment in the case of the vitronectin, the results obtained with the ELISA assay (used to measure the quantity of VN in the supernatant solutions) show significant variability. In fact, repeated analyses of the same supernatant sample using the ELISA method described above, lead to a certain level of discrepancy, suggesting that the ELISA assay itself could certainly be the source of such variability. The kinetics of the recovered release profiles was nevertheless consistent for all samples.

### *2. Release from Pluronic UV-cross-linked microcapsules*

*a. Vitronectin.* The release profile of vitronectin from the UV-cross-linked microparticles is expected to differ from that observed from the cross-linked macrogels, due to the significant increases in available surface area for delivery in the case of the microparticles. The short-term release of encapsulated VN was investigated using the same ELISA technique in both UV-cross-linked DA PF-127 microparticles and macrogels. The particles were collected from the

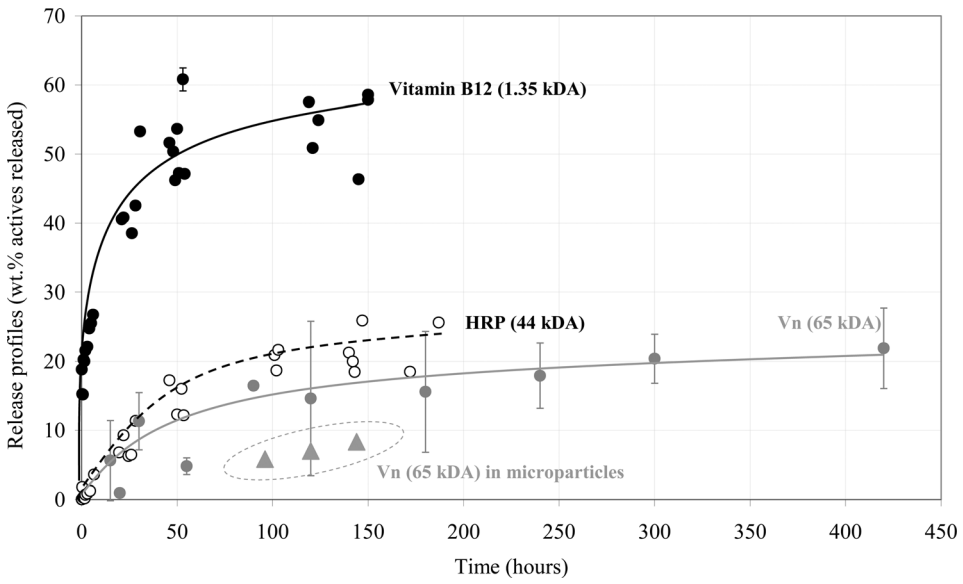


FIG. 10. Release data and profiles for vitronectin (grey line), HRP (dotted line) and vitamin $B_{12}$ (black line), from cross-linked DA PF-127 macro (bulk)-gels. The amount of vitronectin released after 4, 5 and 6 days from DA PF-127 cross-linked microparticles prepared on-chip is reported (triangles) for comparison.

device, dried, and re-suspended in a PBS supernatant solution. No VN was detected, within the detection limit of the ELISA technique in this supernatant solution before 3 days. After 4, 5, and 6 days, the VN concentrations detected in the supernatant solution correspond to 5.5 wt. %, 7 wt. %, and 8.5 wt. % of the encapsulated VN, respectively, as shown in Figure 10. It has to be noted that the VN content of all samples of particles collected from the microfluidic chip for the release studies corresponded to at least 10 000 times the detection limit, once the particles had been re-suspended in the PBS supernatant solution. It has to be noted also that the particles, as well as the macrogels, dissolve to some extent, albeit it slowly, in PBS. After 5 days, approximately 50% of the gel remains, but it was entirely solubilised after a period of 7 days. For this reason, longer-term release studies (>7 days) were not possible for either system under investigation, regardless of the production method.

In the case of the reference Pluronic macrogels, the release results showed that 15%–20% of VN was released during the first 5 h, which can be defined as an initial burst. The release profile then slowed down dramatically to produce a total VN release of 20%–25% after 10 h. A steady state (25%) was attained after 25–48 h. This experiment was repeated over a longer time span (3 days) and the rate of release was similar to that obtained after 48 h (i.e., only 30%–32% of VN released within 78 h).

The VN molecules are mixed in the reactive polymer solution before the cross-linking occurs and the acrylate groups can potentially react with unpaired cysteine groups in the VN.[51] Two of the 14 cysteine residues in vitronectin are free (Cys-411 and Cys-196) but are in buried positions. The rest form 6 disulfide bonds in the protein. The pKa of a thiol group in a protein is $\sim 8$ and the *p*H of the solution was adjusted to 3.5 to lower the risk of such a reaction. Also, the same reaction would also happen in the case of the bulk gels and would affect the release profile similarly. Here, the relative profiles seem to indicate that Pluronic macrogels and the Pluronic microparticles have different microstructures. In particular, the dense shell-like structure of the microparticles does not exist in the bulk macrogels and would certainly result in major differences in release kinetics, depending on the molecular size of the encapsulant. To investigate the effect of the size of the active on the release profile from the Pluronic microparticles, we studied the release of the vitamin $B_{12}$ molecules.

*b. Vitamin B12 ($VB_{12}$).* The release profiles of $VB_{12}$ molecules encapsulated in UV-cross-linked DA-PF68 macrogels and in UV-cross-linked DA-PF68 microparticles produced in the microfluidic device are shown in Figure 11. The curves are quite different. In the case of the

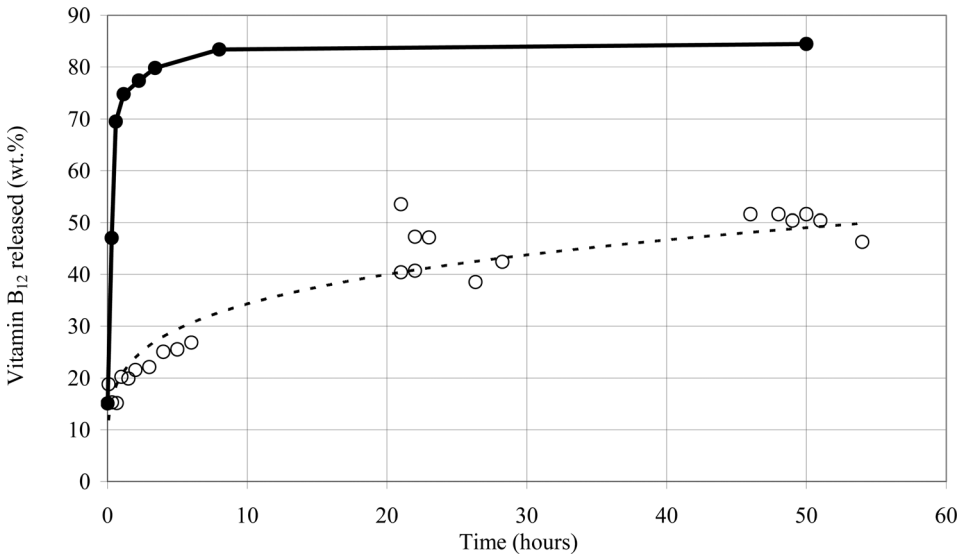


FIG. 11. Release profiles for Vitamin $B_{12}$ encapsulated in cross-linked DA PF-68 macrogels (open symbols, dotted line) and in the case of cross-linked DA PF-68 particles produced within the microfluidic device (solid symbols, full line).

microparticles, the release profile shows a distinct burst: 60% of the encapsulated $VB_{12}$ is released after the first hour. The release slows down and reaches a plateau value at 83% after 8 h. In the case of the macrogels, there is also an initial burst, but only 20% of the encapsulated vitamin molecules are released after 1 h. The curve evolves progressively, reaching a value corresponding to 50% of the encapsulated $VB_{12}$ after 60 h but does not reach a plateau within the period of time investigated. These results indicate that in the case of the small vitamin molecules, release from the particles is much faster than for macro-gels. This is expected when considering the higher surface-to-volume ratio of the particles, but could also be the result of the core-shell morphology of the microparticles. In the case of the macrogels, the vitamin molecules encapsulated in the bulk have to diffuse through to the surface before being leached into the supernatant solution.

These results confirm that any differences in microstructure and format (i.e., bulk gel versus microparticle) between these two systems can affect differences in the release of the encapsulated active molecules, depending on their size. The structure of the microparticles is denser and there is a size cut-off, above which the release is significantly inhibited, an outcome that does not exist in the case of a gel (composed of the same concentration of Pluronic) when presented in a macro-format. This result in particular may be of great interest, as the microparticles of Pluronic, when made using this single step continuous process, would allow two different kinds of molecules to be encapsulated and selectively released over two very different timescales.

## IV. CONCLUSIONS

In this work, we have described a microfluidic technique for the continuous production of multi-layered microparticles. While this work focused on amphiphilic tri-block copolymers of PEO-PPO-PEO, this novel method is highly flexible and can be applied to a wide range of biologically derived or synthetic polymers. The same fabrication scheme was shown to allow for the production of dissimilar particles with varying size, composition, porosity, or internal structure. In particular, different initiation methods for the cross-linking reaction gave rise to different internal morphologies of the produced particles. In the case of multilayered or coated particles, their surface morphology was observed to vary, depending on the nature of the outermost polymer layer. Using labelled protein molecules, we have proven that this technique allows for the encapsulation of active agents in the particles, without any additional processing steps. We have studied the release of a number of different molecules from cross-linked particles produced on-chip as well as from macro hydrogels, composed of the same concentration of polymer. Preliminary results indicate that the release from macro-hydrogels depends significantly on the size of the encapsulated molecules. Also, the comparison of the release of Vitamin $B_{12}$ from microparticle and macro Pluronic gels showed that the large surface–to-volume ratio in the case of the microparticles gives rise to a quick burst release of the encapsulated active, whilst the diffusion-dominated release from the macro-gels is progressive. In the case of larger protein molecules, the microparticles retain the deliverables and the release is slower from the particles than from bulk gels. The ability of the particles of retaining large deliverable molecules until they degrade, whilst allowing for the fast release of other small deliverable molecules, is of great interest. The tuning of the local density of the cross-linked polymer from which these microparticles are composed, and the capability to introduce a number of alternate polymer layers which have their own intrinsic delivery characteristics, provides significant flexibility in tailoring the delivery "cut-off sizes" of such microparticle systems.

## ACKNOWLEDGMENTS

The authors would like to acknowledge the funding from the ARC Linkage Grants Scheme (LP0562505) and the advice received from Professor Zee Upton, Chief Scientific Officer of Tissue Therapies Ltd., the industrial partner in this project. The authors especially thank Dr. Tim Dargaville (Queensland University of Technology, Brisbane) for his assistance with the synthesis of the diacrylated pluronic polymers, as well as with the optimization of the ELISA assay, which had to be specifically adapted for the study of the release of Vitronectin.

[1]S. Freiberg and X. X. Zu, Int. J. Pharmacol. **282**, 1–18 (2004).
[2]P. Burey, B. R. Bhandari, T. Howes, and M. J. Gidley, Crit. Rev. Food Sci. Nutr. **48**, 361–377 (2008).
[3]D. Missirlis, N. Tirelli, and J. A. Hubbell, Langmuir **21**, 2605–2613 (2005).
[4]A. Nagayasu, K. Uchiyama, and H. Kiwada, Adv. Drug Delivery Rev. **40**, 75–87 (1999).
[5]T. Nakashima, M. Shimizu, and M. Kukizaki, Adv. Drug Delivery Rev. **45**, 47–56 (2000).
[6]N. Elvassore, M. Baggio, P. Palladdo, and A. Bertucco, Biotechnol. Bioeng. **73**, 450–457 (2001).
[7]G. B. Sukhorukov, D. V. Volodkin, A. M. Gunther, A. I. Petrov, D. B. Shenoy, and H. Mohwald, J. Mater. Chem. **14**, 2073–2081 (2004).
[8]A. J. P. Santinho, J. M. Ueta, O. Freitas, and N. L. Pereira, J. Microencapsul. **19**, 549–558 (2002).
[9]K. K. Nishi and A. Jayakrishnan, Biomacromolecules **5**(4), 1489–1495 (2004).
[10]G. Fundueanu, M. Constantin, F. Bortolotti, P. Ascenzi, R. Cortesi, and E. Menegatti, Macromol. Biosci. **5**, 955–954 (2005).
[11]D. J. McClements, E. A. Decker, Y. Park, and J. Weiss, Crit. Rev. Food Sci. Nutr. **49**, 577–606 (2009).
[12]T. Thorsen, R. W. Roberts, F. H. Arnold, and S. R. Quake, Phys. Rev. Lett. **86**, 4163–4166 (2001).
[13]T. Nisisako, T. Torii, and T. Higuchi, Lab Chip **2**, 24–26 (2002).
[14]H. Zhang, E. Tumarkin, E. Peerani, Z. Nie, R. M. A. Sullan, G. C. Walker, and E. Kumacheva, J. Am. Chem. Soc. **128**, 12205–12210 (2006).
[15]K.-S. Huang, T.-H. Lai, and Y.-C. Lin, Lab Chip **6**, 954–957 (2006).
[16]K. Liu, H.-J. Ding, J. Liu, Y. Chen, and X.-Z. Zhao, Langmuir **22**, 9468–9472 (2006).
[17]S. Sugiura, T. Oda., Y. Izumida, Y. Aoyagi, M. Satake, A. Ochiai, N. Ohkohchi, and M. Nakajima Biomaterials **26**, 3327–3331 (2005).
[18]M. Zourob, S. Mohr, A. G. Mayes, A. Macaskill, N. Pérez-Moral, P. R. Fielden, and N. J. Goddard, Lab Chip **6**, 296–301 (2006).
[19]M. Seo, Z. Nie, S. Xu, M. Mok, P. C. Lewis, R. Graham, and E. Kumacheva, Langmuir **21**, 11614–11622 (2005).
[20]P. C. Lewis, R. R. Graham, Nie Z., S. Xu, M. Seo, and E. Kumacheva, Macromolecules **38**, 4536–4538 (2005).
[21]Z. Nie, S. Xu, M. Seo, P. C. Lewis, and E. Kumacheva, J. Am. Chem. Soc. **127**, 8058–8063 (2005).
[22]Q. B. Xu, M. Hashimoto, T. T. Dang, T. Hoare, D. S. Kohane, G. M. Whitesides, R. Langer, and D. G. Anderson, Small **5**, 1575–1581 (2009).
[23]D. R. Link, S. L. Anna, D. A. Weitz, and H. A. Stone, Phys. Rev. Lett. **92**, 054503 (2004).
[24]C. H. Yeh, Q. L. Zhao, S. J. Lee, and Y. C. Lin, Sens. Actuators, A **151**, 231–236 (2009).
[25]S. L. Anna, N. Bontoux, and H. A. Stone, Appl. Phys. Lett. **82**, 364–366 (2003).
[26]T. Wu, Y. Mei, J. T. Cabral, C. Xu, and K. L. Beers, J. Am. Chem. Soc. **126**, 9880–9881 (2004).
[27]T. Nisisako, T. Torii, and T. Higuchi, Chem. Eng. J. **101**, 23–29 (2004).
[28]S. Freitas, H. P. Merkle, and B. Gander, J. Controllled Release **102**, 313–332 (2005).
[29]T. Higuchi, H. Yabu, and M. Shimomura, Colloids Surf., A **284–285**, 250–253 (2006).
[30]N. Saito, Y. Kagari, and M. Okubo, Langmuir **22**, 9397–9402 (2006).
[31]C. Esen, T. Kaiser, M. A. Borchers, and G. Schweiger, Colloid Polym. Sci. **275**, 131–137 (1997).
[32]I. Cohen, H. Li, J. L. Hougland, M. Mrksich, and S. R. Nagel, Science **292**, 265–267 (2001).
[33]S. Abraham, E. H. Jeong, T. Arakawa, S. Shoji, K. C. Kim, I. Kim, and J. S. Go, Lab Chip **6**, 752–756 (2006).
[34]B. G. De Geest, J. P. Urbanski, T. Thorsen, J. Demeester, and S. C. De Smedt, Langmuir **21**, 10275–10279 (2005).
[35]C. Serra, N. Berton, M. Bouquey, L. Prat, and G. Hadziioannou, Langmuir **23**, 7745–7750 (2007).
[36]W. J. Jeong, J. Y. Kim, J. Choo, E. K. Lee, C. S. Han, D. J. Beebe, G. H. Seong, and S. H. Lee, Lamgmuir **21**, 3738–3741 (2005).
[37]D. Dendukuri, K. Tsoi, T. A. Hatton, and P. S. Doyle, Langmuir **21**, 2113–2116 (2005).
[38]S. Xu, Z. Nie, M. Seo, P. Lewis, E. Kumacheva, H. A. Stone, P. Garstecki, D. B. Weibel, I. Gitlin, and G. M. Whitesides, Angew. Chem. Int. Ed. **44**, 724–728 (2005).
[39]J.-W. Kim, A. S. Utada, A. Fernandez-Nieves, Z. Hu, and D. A. Weitz, Angew. Chem. Int. Ed. **46**, 1819–1822 (2007).
[40]E. Rondeau and J. J. Cooper-White, Langmuir **24**, 6937–6945 (2008).
[41]F. Cellesi, N. Tirelli, and J. A. Hubbell, Macromol. Chem. Phys. **203**, 1466–1472 (2002).
[42]S.-P. Zhao, L.-M. Zhang, D. Ma, C. Yuang, and L. Yang, J. Phys. Chem. B **110**, 16503–16507 (2006).
[43]S.-Y. Lee, G. Tae, and Y. H. Kim, J. Biomater. Sci. Polym. Ed. **18**, 1335–1353 (2007).
[44]S.-Y. Lee and G. Tae, J. Controlled Release **119**, 313–319 (2007).
[45]K. W. Chun, J. B. Lee, S. H. Kim, and T. G. Park, Biomaterials **26**, 3319–3326 (2005).
[46]J. B. Lee, J. J. Yoon, D. S. Lee, and T. G. Park, J. Biomater. Sci., Polym. Ed. **15**, 1571–1583 (2004).
[47]W. Zu and J. Ding, J. Appl. Polym. Sci. **99**, 2375–2383 (2005).
[48]W. Li, Z. Nie, H. Zang, C. Paquet, M. Seo, P. Garstecki, and E. Kumacheva, Langmuir **23**, 8010–8014 (2007).
[49]L.-Y. Chu, A. S. Utada, R. K. Shah, J.-W. Kim, and D. A. Weitz, Angew. Chem. Int. Ed. **46**, 8970–8974 (2007).
[50]D. L. Elbert, A. B. Pratt, M. P. Lutolf, S. Halstenberg, and J. A. Hubbell, J. Controlled Release **76**, 11–25 (2001).
[51]P. van de Wetering, A. T. Metters, R. G. Schoenmakers, and J. A. Hubbell, J. Controlled Release **102**, 619–627 (2005).